CIRP Annals - Manufacturing Technology 00 (2026) 1–6

Contents lists available at ScienceDirect

CIRP Annals - Manufacturing Technology

journal homepage: https://www.editorialmanager.com/CIRP/default.aspx

Tchebychev-based modal-domain coupling (TMDC) for prediction of microtool-tip dynamics

O. Burak Ozdoganlar[a,b,*], Shivang Shekhar[a], Alec Vucsko[a], Kadir Kiran[c], Bekir Bediz[d]

[a] Department of Mechanical Engineering, Carnegie Mellon University, Pittsburgh, Pennsylvania 15213, USA
[b] Departments of Materials Science & Engineering, and Biomedical Engineering, Carnegie Mellon University, Pittsburgh, Pennsylvania 15213, USA
[c] Department of Aircraft Maintenance and Repair, School of Civil Aviation, Suleyman Demirel University, 32700, Isparta, Turkiye
[d] Mechatronics Engineering Program, Faculty of Engineering and Natural Sciences, Sabanci University, Istanbul 34956, Turkey

Submitted by Alkan Donmez (1), Gaithersburg, USA

ARTICLE INFO

Article history:
Available online xxx

Keyword:
Micro-machining stability
Modal-domain coupling
Tool-tip Dynamics

ABSTRACT

Accurate representation of tool-tip dynamics is essential for predicting stability in micromachining. Frequency-domain coupling approaches amplify measurement noise due to matrix inversions and finite-difference approximations of rotational frequency response functions (FRFs). We propose Tchebychev-based modal-domain coupling (TMDC), which represents measured spindle–artefact mode shapes in a Tchebychev basis, evaluates slopes with spectral differentiation, couples a Tchebychev-based tool-dynamics model, and enforces interface compatibility in modal coordinates. TMDC is validated on two ultra-high-speed spindles, showing agreement with measured FRFs up to 15 kHz and avoiding the artificial antiresonances observed with receptance coupling substructure analysis (RCSA). Predicted tool-tip receptances are then used to predict stability for two micro-endmill geometries.

1. Introduction

Tool-tip dynamics govern stability and precision in micromachining [1]. While impact testing can identify tool-tip dynamics, it requires repeated modal tests for each tool–spindle setup and is impractical for microscale tools because of their small size and fragility [2]. A common alternative is a hybrid strategy combining experimentally identified spindle/machine dynamics with analytical or numerical tool models. After a single modal test to identify spindle dynamics up to the spindle nose, tool-tip FRFs for arbitrary microtools can then be predicted by updating only the tool model, without repeating spindle testing. In conventional machining, FRF generation is commonly achieved with Receptance Substructure Analysis (RCSA), a computationally efficient frequency-domain approach [3–9]. RCSA relies on direct tool-tip FRFs, matrix inversions, finite-difference estimates of rotational FRFs, and calibrated interface parameters [10–14]. These requirements are problematic in micromachining, where small tools and ultra-high-speed (UHS) (>60,000 rpm) spindles require broadband predictions to capture responses at multiples of the tooth-passing frequency. As a result, RCSA-based tool-tip FRFs for microtools are often noisy, bandwidth-limited, and contaminated by inversion-induced artefacts.

In this work, we introduce Tchebychev-based modal-domain coupling (TMDC) to predict microtool-tip dynamics while avoiding key limitations of RCSA. TMDC represents experimentally identified spindle dynamics and the tool-dynamics models in *modal* coordinates (natural frequencies, damping ratios, and mode shapes), enforces interface compatibility in the modal domain, and transforms the coupled response back to the physical domain. While modal-domain coupling has been used in other substructuring contexts, its application to tool-tip FRF prediction has been limited because its accuracy depends on the fidelity of experimentally extracted mode shapes and on the computation of smooth spatial derivatives required for slope continuity [15,16]. In TMDC, each experimentally identified mode shape is only available at specific axial measurement locations along the artefact. We therefore approximate each mode-shape with a truncated series of Tchebychev polynomials after mapping the axial coordinate to the interval [−1,1]. This provides a smooth global representation of the mode shapes, and the corresponding axial slopes needed for interface compatibility are obtained by applying a spectral differentiation matrix to the fitted polynomial coefficients, offering derivative estimates that are much more noise-robust than finite-difference differentiation of measured FRFs. This unified representation is consistently used for artefact removal and tool addition, ensuring that displacement and slope continuity are maintained on the same basis without introducing additional calibrated interface parameters.

A recent study [12] examined tool-tip dynamics in micromachining across different spindle speeds and microtool geometries, including an empirical analysis of speed-induced mode splitting. In contrast, this paper analyzes and validates the coupling-decoupling methodology that enables reliable, high-bandwidth tool-tip FRF synthesis. Specifically, it introduces a modal-domain formulation that

* Corresponding author.
E-mail address: burakoz@andrew.cmu.edu (O.B. Ozdoganlar).

https://doi.org/10.1016/j.cirp.2026.04.054

Please cite this article as: O.B. Ozdoganlar et al., Tchebychev-based modal-domain coupling (TMDC) for prediction of microtool-tip dynamics, CIRP Annals - Manufacturing Technology (2026), https://doi.org/10.1016/j.cirp.2026.04.054

represents experimentally identified spindle-artefact mode shapes using a global Tchebychev basis and calculates interface slopes through spectral differentiation. By avoiding finite-difference rotational FRFs and ill-conditioned frequency-domain inversions, the method enhances numerical robustness and usable coupling bandwidth compared to RCSA. Unlike [12], the focus here is on direct comparison with RCSA, smoother rotational FRFs, demonstration of both coupling and decoupling, and evaluation of the resulting tool-tip FRFs and stability diagrams.

TMDC is validated on two UHS spindles using precision artifacts and microtools with varied overhangs, showing high-bandwidth agreement between predicted and measured dynamics. The predicted tool-tip receptance matrix is then used to generate stability limit diagrams for UHS micromachining. These results show that tool-tip FRF prediction can be carried out robustly in the modal domain when experimentally identified spindle-artefact modes are represented in a Tchebychev basis and differentiated spectrally, enabling consistent artefact removal and tool addition without ill-conditioned inversions or interface-parameter calibration.

2. Prediction of tool-tip dynamics

For micromachining, our TMDC approach predicts the tool-tip dynamics using a hybrid strategy that couples experimentally identified spindle dynamics with an analytical tool model in the modal domain (Fig. 1). The spindle is identified from multi-point modal testing of a spindle-artefact assembly, and the artefact is removed by modal-domain decoupling to recover spindle dynamics at the spindle nose. The tool model is then coupled by enforcing displacement and slope continuity at the interface to obtain the tool-tip FRFs.

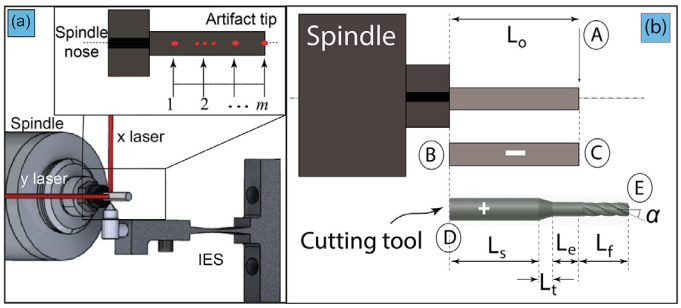

Fig. 1. (a) Spindle identification: the impact excitation system (IES) excites the artefact at position 1; responses measured at m locations. (b) Tool-tip prediction: decouple artefact B–C to obtain spindle dynamics at D, then couple tool model D–E to predict tool-tip dynamics.

2.1. Modelling of cutting tools

The TMDC approach depends on accurate modelling of microtool dynamics. To obtain the tool-tip dynamics for any tool or artefact, we use the spectral–Tchebychev (ST) formulation introduced in [17,18]. Briefly, the tool is modelled as a piecewise Timoshenko beam with spatially varying cross-sectional area, moments of inertia, and mass per unit length, capturing bending–shear coupling and rotary inertia effects that become significant for short, tapered geometries. Using Hamilton's principle, the strain and kinetic energies are formulated and discretized along the beam axis to obtain the governing equations in terms of the displacement field $q(z)$ and its spatial derivatives along the tool axis z (normalized to be $z \in [-1, 1]$).

The ST technique represents $q(z)$ using a truncated (n-term) Tchebychev expansion as

$$q(z) = \sum_{k=0}^{n-1} a_k \tau_k(z), \tag{1}$$

where $\tau_k(z) = \cos(k\ cos^{-1}(z))$ are Tchebychev polynomials and a_k are Tchebychev coefficients. In vector-matrix notation, this can be represented as $\boldsymbol{q} = \Gamma_F \boldsymbol{a}$ and the corresponding mapping $\boldsymbol{a} = \Gamma_B \boldsymbol{q}$, where Γ_F and Γ_B are the forward and backward transformation matrices between the Tchebychev and physical coordinates [17]. Tchebychev expansion enables direct evaluation of spatial derivatives via spectral differentiation matrices, $\boldsymbol{Q}^{(d)}$, as $\boldsymbol{q}^{(d)} = \boldsymbol{Q}^{(d)}\boldsymbol{q}$, where d denotes the order of spatial differentiation. Using these expansions, the system matrices are assembled efficiently (via inner-product matrices) [19]. Solving the resulting free–free eigenvalue problem yields the natural frequencies and mode shapes required for modal-domain coupling.

2.2. Experimental characterization of spindle dynamics

To identify the dynamics of UHS spindles, a testbed comprising a custom flexure-guided impact excitation system (IES) and two laser Doppler vibrometers (LDVs) for non-contact measurements was developed (Fig. 2). A precision cylindrical artefact was mounted to the spindle and excited at multiple axial locations (Fig. 1a) using the IES, while the LDVs measured the resulting vibrations in two orthogonal directions. The resulting multi-point FRFs enable the extraction of the spindle–artefact mode shapes for high-fidelity characterization over a broad frequency range [20].

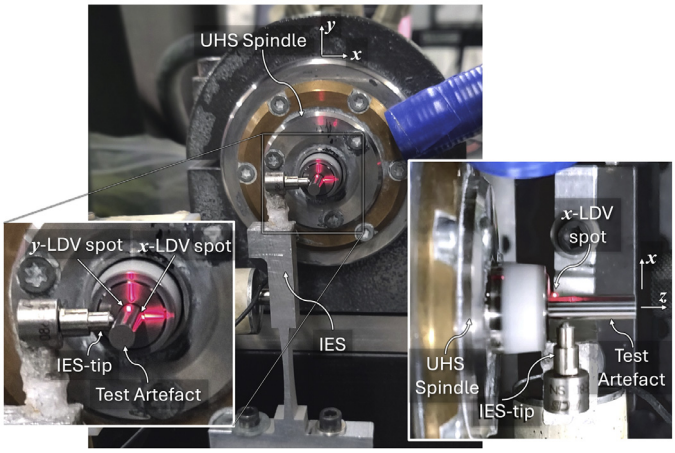

Fig. 2. Testbed for experimental identification of spindle-artefact dynamics and for experimental validations.

The measured multi-point FRFs were processed using a polyreference frequency-domain modal estimator (PolyMAX) to extract modal parameters. Each identified mode shape $\phi_k(z)$ is then approximated using a truncated Tchebychev expansion (order $n < m$), where n was selected by minimizing the normalized reconstruction error of the measured mode-shape samples, yielding a smooth representation and a corresponding set of coefficients for the N_m retained modes. The corresponding coefficient vectors are stacked to form the $n \times N_m$ coefficient matrix $\boldsymbol{A}$. The mode shape samples at the measurement locations are recovered as $\boldsymbol{\phi} = \Gamma_B \boldsymbol{A}$. From this, the spatial derivatives are evaluated using spectral differentiation. Since the displacement field is represented using the Tchebychev polynomials, the geometric constraints can be applied via the differentiation matrix $\boldsymbol{Q}^{(d)}$. This provides a consistent basis for the decoupling and coupling steps described next while reducing sensitivity to noise.

2.3. Modal domain coupling

TMDC assembles spindle–artefact and tool dynamics by enforcing interface compatibility directly in the modal domain. Each substructure s (i.e., measured spindle–artefact, artefact to be removed, and the tool model) is represented by a truncated, mass-normalized modal matrix $\boldsymbol{\phi}_s$ with modal coordinates $\boldsymbol{\eta}_s$, such that $\boldsymbol{q}_s = \boldsymbol{\phi}_s \boldsymbol{\eta}_s$, where $\boldsymbol{q}_s$ includes the translational and rotational displacement degrees of freedom (DOF), including at the coupling locations. Stacking the substructures yields

$$\boldsymbol{q} = \boldsymbol{\Phi}\boldsymbol{\eta}, \boldsymbol{\Phi} = \mathrm{diag}(\boldsymbol{\phi}_1, \boldsymbol{\phi}_2, \boldsymbol{\phi}_3), \boldsymbol{\eta} = \left[\boldsymbol{\eta}_1^{\mathrm{T}} \boldsymbol{\eta}_2^{\mathrm{T}} \boldsymbol{\eta}_3^{\mathrm{T}}\right]^{\mathrm{T}}. \tag{2}$$

The identified experimental modes are scaled using the extracted modal constants (residues) so that each mode is mass-normalized

Please cite this article as: O.B. Ozdoganlar et al., Tchebychev-based modal-domain coupling (TMDC) for prediction of microtool-tip dynamics, CIRP Annals - Manufacturing Technology (2026), https://doi.org/10.1016/j.cirp.2026.04.054

prior to coupling. This diagonalizes the mass and stiffness matrices. For removing the artefact dynamics, we assemble the mass ($\boldsymbol{M}$) and stiffness ($\boldsymbol{K}$) matrices as

$$\boldsymbol{M} = \mathrm{diag}(\boldsymbol{I}_1, -\boldsymbol{I}_2, \boldsymbol{I}_3), \quad \boldsymbol{K} = \mathrm{diag}(\boldsymbol{\Omega}_1^2, -\boldsymbol{\Omega}_2^2, \boldsymbol{\Omega}_3^2), \tag{3}$$

where $\boldsymbol{I}_s$ is the identity matrix and $\boldsymbol{\Omega}_s$ is the diagonal matrix of natural frequencies for substructure s. The negative sign mathematically negates the artefact's energy contribution, effectively subtracting it from the assembly to isolate the spindle; this approach is numerically stable when the removed substructure is represented with the same modal bandwidth. Damping is accounted for using the experimentally identified modal damping ratios for the kth mode, obtained from experimental characterization with the artefact.

To couple or decouple the substructures, displacement and slope (rotation) continuity must be enforced at the interface points in physical coordinates. Those compatibility conditions can be written as $q_A = q_C$, $q_B = q_D$, $q'_A = q'_C$, and $q'_B = q'_D$, where prime indicates spatial derivative, and the subscripts A, B, C, and D denote the locations of the coupling points of the substructures (see Fig. 1b). These compatibility equations can be written in matrix form as $\overline{\boldsymbol{B}}\boldsymbol{q} = \overline{\boldsymbol{B}}\ \boldsymbol{\Phi}\ \boldsymbol{\eta} = \boldsymbol{0}$, where $\overline{\boldsymbol{B}}$ is the constraint matrix constructed from the compatibility equations shown above.

To enforce the constraints, we map the modal coordinates using a projection matrix $\overline{\boldsymbol{P}}$ spanning the null space of $\overline{\boldsymbol{B}}\boldsymbol{\Phi}$ such that $\boldsymbol{\eta} = \overline{\boldsymbol{P}}\ \boldsymbol{\xi}$, where $\boldsymbol{\xi}$ are the mapped coordinates that satisfy the constraints. Using these, the equations of motion for the global system that satisfy the compatibility conditions can now be written as $\boldsymbol{M}_\xi\ddot{\boldsymbol{\xi}} + \boldsymbol{K}_\xi\boldsymbol{\xi} = \boldsymbol{0}$, where $\boldsymbol{M}_\xi = \overline{\boldsymbol{P}}^T\boldsymbol{M}\overline{\boldsymbol{P}}$, and $\boldsymbol{K}_\xi = \overline{\boldsymbol{P}}^T\boldsymbol{K}\overline{\boldsymbol{P}}$. The modal parameters of the assembled system can be obtained using eigenvalue analysis. Once the solution $\boldsymbol{\xi}$ is found, the physical-domain coordinates can be obtained as $\boldsymbol{q} = \boldsymbol{\Phi}\overline{\boldsymbol{P}}\boldsymbol{\xi}$. Artefact removal and tool addition are handled consistently by selecting the appropriate substructures and signs in $\boldsymbol{M}$ and $\boldsymbol{K}$.

2.4. Receptance matrix at the tool-tip

To generate stability diagrams, tool-tip displacement-to-force ($\boldsymbol{H}$) (translational) FRFs of the coupled spindle–tool assembly are required. In RCSA, the coupling/decoupling procedure requires the use of translational–rotational subreceptances, including the slope-to-force ($\boldsymbol{N}$), displacement-to-moment ($\boldsymbol{L}$), and slope-to-moment ($\boldsymbol{P}$) subreceptances. These are typically obtained using finite-difference differentiation, which can amplify noise. In contrast, TMDC predicts tool-tip FRFs directly from the coupled modal model; if slope/rotation terms are needed, they are obtained from the same coupled mode shapes using spectral differentiation in the global Tchebychev basis (e.g., $\boldsymbol{q}' = \boldsymbol{Q}^{(1)}\boldsymbol{q}$), avoiding finite-difference operations. Thus, the subreceptances are computed without finite-difference operations.

The receptance between a force applied at DOF j and the response measured at DOF i is obtained by modal summation. Assuming reciprocity (i.e., symmetry), $\boldsymbol{H}$, $\boldsymbol{N}$, $\boldsymbol{L}$, $\boldsymbol{P}$, and the assembled receptance matrix at the tool tip, $\boldsymbol{R}_{tt}$, can be given as

$$H_{ij}(\omega) = \sum_{k=1}^{N_m} \frac{q_{i,k}\, q_{j,k}}{D_k(\omega)},\ L_{ij}(\omega) = \sum_{k=1}^{N_m} \frac{q_{i,k}\, q'_{j,k}}{D_k(\omega)} = N_{ji}(\omega),\ P_{ij}(\omega) = \sum_{k=1}^{N_m} \frac{q'_{i,k}\, q'_{j,k}}{D_k(\omega)}, \tag{4}$$

$$D_k(\omega) = -\omega^2 + 2j\ \zeta_k\omega\ \omega_{n,k} + \omega_{n,k}^2, \tag{5}$$

$$\boldsymbol{R}_{tt} = \begin{bmatrix} H_{tt} & L_{tt} \\ N_{tt} & P_{tt} \end{bmatrix}. \tag{6}$$

Here, $\omega_{n,k}$ and ζ_k are the natural frequency and damping ratio of the k-th coupled mode, and $q_{i,k}$ denotes the i-th component of the k-th assembled mode-shape vector evaluated at the selected physical DOFs (translations and slopes/rotations) used to form the tool-tip receptance matrix. Importantly, unlike RCSA, TMDC predicts the tool-tip FRFs directly from the coupled modal model and does not require the $\boldsymbol{N}$, $\boldsymbol{L}$, and $\boldsymbol{P}$ subreceptance matrices. They are computed here only for one-to-one comparison with RCSA.

The TMDC tool model applies to arbitrary microtool geometries, including varying diameters and tapered profiles. However, significant changes in shank diameter or clamping conditions require re-identification of the spindle dynamics at the interface.

3. Results and discussion

3.1. Validation on two UHS spindles

In this section, we experimentally validate the translational FRFs. Rotational subreceptances are computed using spectrally differentiated mode shapes, which avoids the numerical noise amplification associated with finite-difference differentiation.

TMDC was first validated using a ceramic-bearing UHS spindle (SC1060A, Fischer Precise). A cylindrical artefact with an overhang length of 19 mm was mounted at the spindle nose. Modal testing was conducted on the non-rotating spindle (Fig. 1(a)). The FRFs were measured at m = 17 locations from the spindle nose to the artefact tip (Fig. 3). Using these measurements, two additional overhang configurations were obtained: (1) the 19 mm artefact was removed, and a 6 mm cylinder was coupled to obtain a reduced overhang, and (2) a 14 mm cylinder was added to obtain a 33 mm overhang. The predicted FRFs (H_{xx}) in Figs. 4 and 5 show good agreement with measurements for the longer overhang and acceptable agreement for the shorter overhang, with resonance peaks captured within 40–420 Hz (≤5% error) and within ±2 dB in magnitude, confirming that TMDC accurately reproduces the spindle–artefact dynamics across overhang configurations.

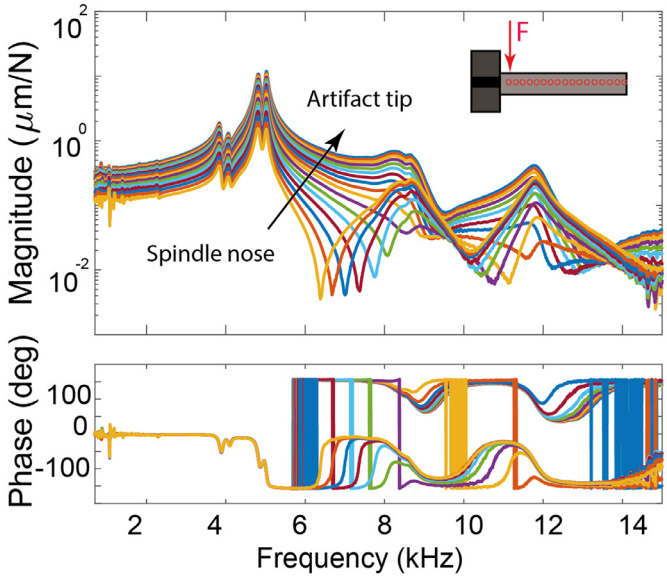

Fig. 3. FRFs obtained on different (H_{j1}) points on a ceramic bearing spindle. H_{j1} represents the excitation location *1* and varying measurement locations *j* in x direction.

Next, TMDC was applied to an air-bearing spindle (ASC 200, Fischer Precise). Tests were performed on a 12 mm overhang artefact at m = 12 locations. The measured configuration was then modified by (1) removing the 12 mm cylinder and coupling a 2 mm cylinder to represent the dynamics at the spindle nose and (2) coupling a standard micro-endmill, for a total overhang of 19 mm.

For comparison, RCSA was implemented following [7]. Because RCSA requires impact excitation at the tool/artefact tip, a separate test configuration was used to avoid low signal levels associated with longer, more flexible artefacts. Thus, the spindle receptance for RCSA was identified using a 5 mm artefact. An inverse RCSA procedure was then employed to estimate the spindle dynamics for a 2 mm overhang before adding the micro-endmill. For a one-to-one comparison, we report the full tool-tip receptance matrix; for TMDC, the $\boldsymbol{N}$, $\boldsymbol{L}$, and $\boldsymbol{P}$ are calculated from the coupled modes (not required for coupling). As shown in Figs. 6 and 7, the reconstructed spindle-tool assembly dynamics from the TMDC approach exhibit substantially reduced

Please cite this article as: O.B. Ozdoganlar et al., Tchebychev-based modal-domain coupling (TMDC) for prediction of microtool-tip dynamics, CIRP Annals - Manufacturing Technology (2026), https://doi.org/10.1016/j.cirp.2026.04.054

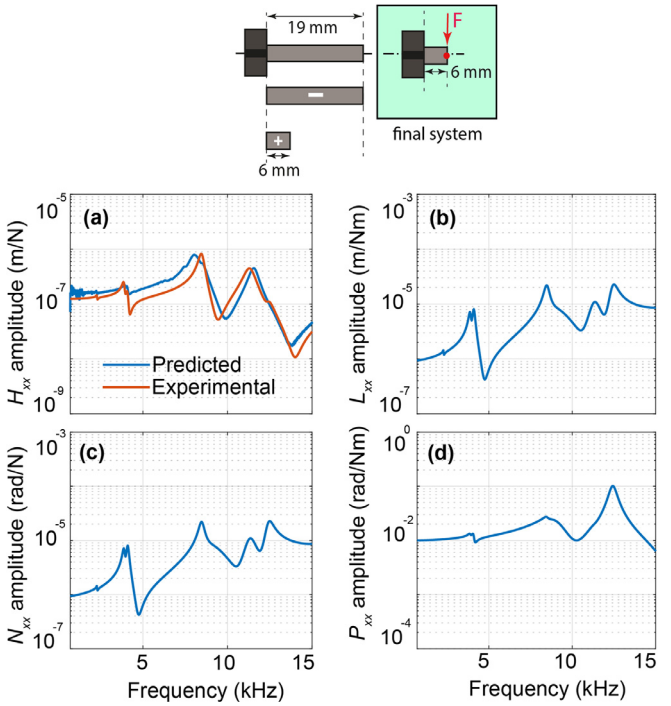

Fig. 4. Receptance matrix (***R***) of the ceramic bearing spindle at a stationary condition for an overhang length of 6 mm.

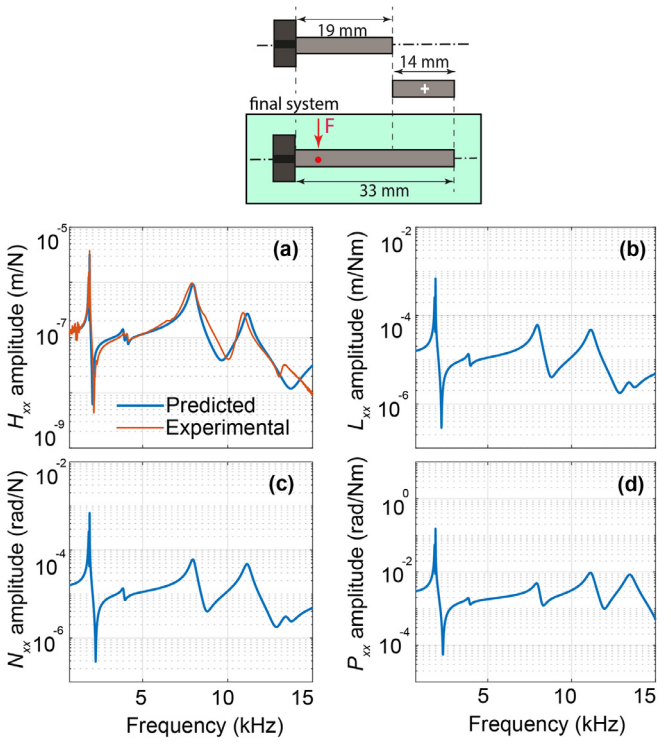

Fig. 5. Receptance matrix (***R***) of the ceramic bearing spindle at a stationary condition for an overhang length of 33 mm.

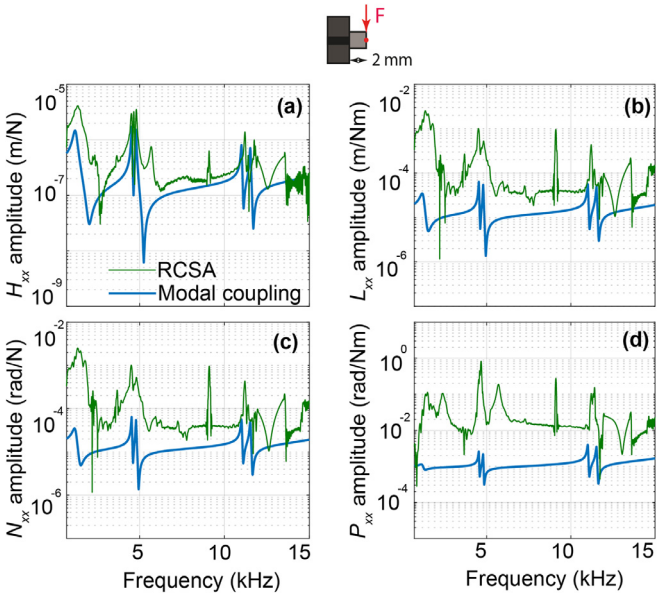

Fig. 6. Receptance matrix (***R***) comparison of the air bearing spindle at 110 krpm for spindle dynamics with a 2 mm overhang.

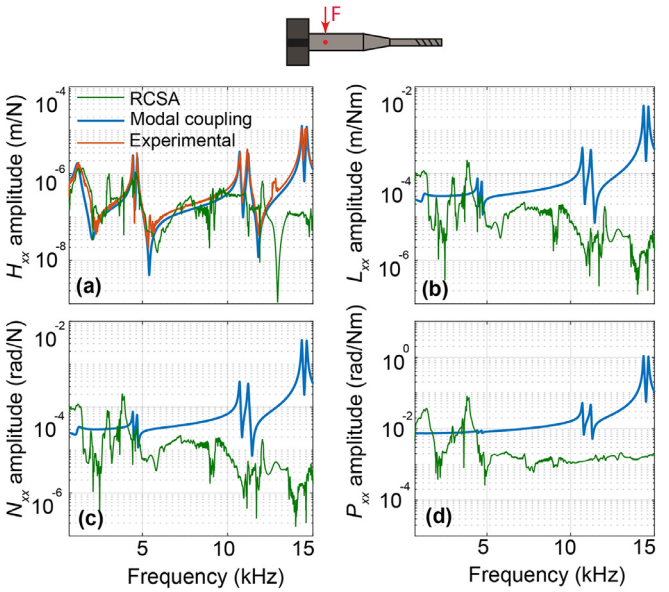

Fig. 7. Receptance matrix (***R***) comparison of the air bearing spindle at 110 krpm for a standard endmill with a 19 mm overhang.

noise and avoid the amplified antiresonances observed in the displacement and rotational FRF predictions using RCSA.

The TMDC-predicted FRF in Fig. 7(a) shows good agreement with the measurements up to 15 kHz: the dominant resonance peaks are captured with an average frequency deviation of 37.2 Hz (max 68 Hz) and a mean amplitude error of 1.10 dB (max 2.21 dB). In contrast, the RCSA predictions begin to deviate significantly beyond 2–3 kHz. Error calculations from Fig. 7a for the entire 15 kHz bandwidth show that, relative to RCSA, the TMDC approach reduces the Least Squares Error (LSE) by 68.3% and the Root Mean Square Error (RMSE) by 43.6%. A close examination indicates that RCSA produces high level of noise as well as many artificial antiresonance and resonance peaks that are not observed in the experimental data. Thus, compared to RCSA, the TMDC method yields more consistent predictions of UHS spindle-microtool-tip dynamics.

3.2. Demonstrative example: stability analyses using tool-tip dynamics from TMDC

To evaluate the stability, tool-tip FRFs were computed for the air-bearing spindle with two tool geometries (standard and long-reach endmills; Table 1) at a spindle speed of 110 krpm. Fig. 8 shows the predicted tool-tip FRFs for the two tools and the stability limit diagrams generated via a Fourier-series-based analytical approach [21] using FRFs calculated from TMDC. We considered down-milling of aluminum with full immersion (cutting-force coefficients for Al: $K_{tc} = 970$ N/mm^2, $K_{rc} = 620$ N/mm^2) [22]. This example demonstrates how TMDC-based tool-tip

Please cite this article as: O.B. Ozdoganlar et al., Tchebychev-based modal-domain coupling (TMDC) for prediction of microtool-tip dynamics, CIRP Annals - Manufacturing Technology (2026), https://doi.org/10.1016/j.cirp.2026.04.054

Table 1
Geometries of the two micro-tools used for tool-tip dynamics (see Fig. 1b).

Endmill	# flute	d_s (mm)	L_s (mm)	L_t (mm)	d_o (μm)	L_e (mm)	L_f (mm)	η (deg.)
Standard	2	3.175	13.6	5.4	811	0	2.7	46.8
Long reach	2	3.175	2.5	4.4	1397	8.5	4.2	46.8

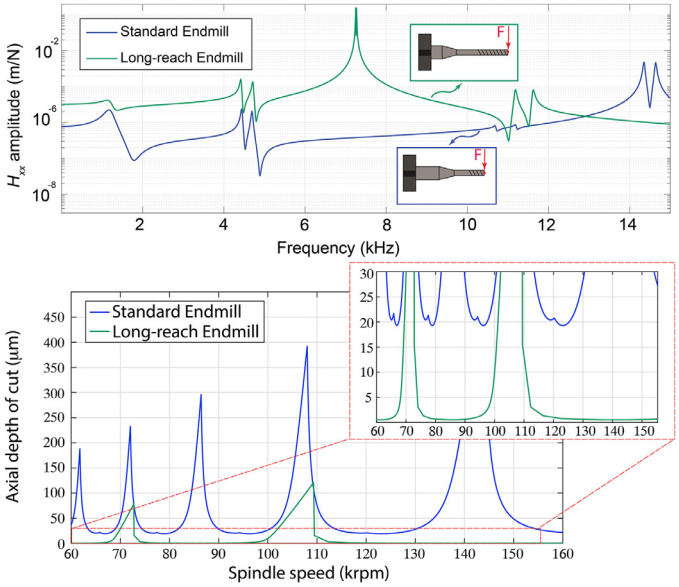

Fig. 8. TOP: Tool-tip FRFs along the x-direction (H_{xx}) for the air bearing spindle with the standard and the long reach endmills at 110 krpm. BOTTOM: Stability limit diagrams for the standard endmill-air bearing spindle and the long reach endmill-air bearing spindle assemblies.

dynamics can be directly translated into stability predictions for UHS micromachining.

4. Summary and conclusion

In this paper, we presented TMDC, a modal-domain coupling framework for predicting and analyzing the tool-tip dynamics of high-speed and UHS spindle–tool systems. The method represents experimentally identified spindle dynamics using a global Tchebychev basis and couples them with analytical microtool models through a unified modal decoupling/coupling procedure. The approach was demonstrated on two UHS spindles using artefacts with different overhang lengths, and the coupled models showed high-bandwidth agreement with measurements (up to 15 kHz). We then used TMDC to compute the complete tool-tip receptance matrix for multiple tool geometries. To demonstrate an application of the TMDC, we generated stability limit diagrams for two tool geometries when mounted on a UHS spindle.

Compared with classical RCSA, the proposed framework offers two main advantages: (1) it improves robustness for microtool applications, where low signal levels and small tool geometries make conventional RCSA particularly error-prone, and (2) it achieves high-bandwidth accuracy without relying on ill-conditioned frequency-domain matrix inversion or finite-difference-based rotational FRFs. Within the scope of high-bandwidth FRF synthesis studied here, TMDC provides a robust alternative to RCSA for microtool-tip dynamics prediction.

Declaration of generative AI and AI-assisted technologies in the manuscript preparation process

During the preparation of this work, the author(s) used Gemini and ChatGPT to proofread the paper. After using this tool/service, the author(s) reviewed and edited the content as needed and take(s) full responsibility for the content of the published article.

Declaration of competing interest

The authors declare that they have no known competing financial interests or personal relationships that could have appeared to influence the work reported in this paper.

CRediT authorship contribution statement

O. Burak Ozdoganlar: Writing – review & editing, Writing – original draft, Supervision, Resources, Project administration, Methodology, Funding acquisition, Conceptualization. **Shivang Shekhar:** Writing – review & editing, Writing – original draft, Visualization, Validation, Software, Methodology, Formal analysis, Data curation. **Alec Vucsko:** Writing – review & editing, Writing – original draft, Visualization, Validation, Formal analysis. **Kadir Kiran:** Visualization, Software, Investigation. **Bekir Bediz:** Writing – review & editing, Writing – original draft, Visualization, Software, Methodology, Formal analysis.

Please cite this article as: O.B. Ozdoganlar et al., Tchebychev-based modal-domain coupling (TMDC) for prediction of microtool-tip dynamics, CIRP Annals - Manufacturing Technology (2026), https://doi.org/10.1016/j.cirp.2026.04.054

References

[1] Quintana G, Ciurana J (2011) Chatter in Machining Processes: A Review. *International Journal of Machine Tools and Manufacture* 51(5):363–376.
[2] Lu X, Jia Z, Liu S, Yang K, Feng Y, Liang SY (2019) Chatter Stability of Micro-Milling by Considering the Centrifugal Force and Gyroscopic Effect of the Spindle. *Journal of Manufacturing Science and Engineering* 141(11):111003.
[3] Schmitz T, Betters E, Budak E, Yuksel E, Park S, Altintas Y (2022) Review and Status of Tool-Tip Frequency Response Function Prediction Using Receptance Coupling. *Precision Engineering* 79:60–77.
[4] Sulitka M, Falta J, Kohut P (2024) Single Artefact Inverse RCSA With Improved Cross-Compliance Identification. *The International Journal of Advanced Manufacturing Technology* 134:5413–5429.
[5] Schmitz T, Cornelius A, Karandikar J, Tyler C, Smith S (2022) Receptance Coupling Substructure Analysis and Chatter Frequency-Informed Machine Learning for Milling Stability. *CIRP Annals – Manufacturing Technology* 71(1):321–324.
[6] Zatarain M (2014) Receptance Coupling for Tool-Point Dynamic Prediction by Fixed Boundaries Approach. *International Journal of Machine Tools and Manufacture* 78:18–29.
[7] Kumar UV, Schmitz TL (2012) Spindle Dynamics Identification for Receptance Coupling Substructure Analysis. *Precision Engineering* 36(3):435–443.
[8] Montevecchi F, Grossi N, Scippa A, Campatelli G (2016) Improved RCSA Technique for Efficient Tool-Tip Dynamics Prediction. *Precision Engineering* 44:152–162.
[9] Park SS, Altintas Y, Movahhedy M (2003) Receptance Coupling for End Mills. *International Journal of Machine Tools and Manufacture* 43(9):889–896.
[10] Ji X, Bi Q, Yu L, Ren F, Wang Y (2020) A Robust RCSA-Based Method for the In Situ Measurement of Rotating Tool-Tip Frequency Response Functions. *Journal of Manufacturing Science and Engineering* 142(8):081004.
[11] Bediz B, Gozen BA, Korkmaz E, Ozdoganlar OB (2014) Dynamics of Ultrahigh-Speed Spindles Used for Micromachining. *International Journal of Machine Tools and Manufacture* 87:27–38.
[12] Shekhar S, Bediz B, Ozdoganlar OB (2023) Tool-Tip Dynamics in Micromachining With Arbitrary Tool Geometries and the Effect of Spindle Speed. *International Journal of Machine Tools and Manufacture* 185:103981.
[13] Zhang J, Schmitz T, Zhao W, Lu B (2011) Receptance Coupling for Tool Point Dynamics Prediction on Machine Tools. *Chinese Journal of Mechanical Engineering-English Edition* 24(3):340.
[14] Chaux JD, Osoro PXA, Arrazola PJ (2025) A Novel Computational Approach Using Receptance Coupling Substructure Analysis for Prediction of Tool Tip Dynamics in Industrial Machining Applications. *International Journal of Machine Tools and Manufacture* 209:104296.
[15] de Klerk D, Rixen DJ, Voormeeren SN (2008) General Framework for Dynamic Substructuring: History, Review and Classification of Techniques. *AIAA Journal* 46 (5):1169–1181.
[16] Weng S, Zhu H, Xia Y, Li J, Tian W (2020) A Review on Dynamic Substructuring Methods for Model Updating and Damage Detection of Large-Scale Structures. *Advances in Structural Engineering* 23(3):584–600.
[17] Filiz S, Ozdoganlar OB (2008) Microendmill Dynamics Including the Actual Fluted Geometry and Setup Errors—Part I: Model Development and Numerical Solution. *ASME Journal of Manufacturing Science and Engineering* 130(3):031119-1–031119-10.
[18] Bediz B, Ozdoganlar OB (2019) Rotational Dynamics of Micro-Scale Cutting Tools. *Precision Engineering* 60:1–11.
[19] Yagci B, Filiz S, Romero LA, Ozdoganlar OB (2009) A Spectral–Tchebychev Technique for Solving Linear And Nonlinear Beam Equations. *Journal of Sound and Vibration* 321(1–2):375–404.
[20] Bediz B, Korkmaz E, Ozdoganlar OB (2014) An Impact Excitation System for Repeatable, High-Bandwidth Modal Testing of Miniature Structures. *Journal of Sound and Vibration* 333:2743–2761.
[21] Altintas Y, Budak E (1995) Analytical Prediction of Stability Lobes in Milling. *CIRP Annals – Manufacturing Technology* 44(1):357–362.
[22] Shi J, Jin X, Cao H (2022) Chatter Stability Analysis in Micro-Milling With Aerostatic Spindle Considering Speed Effect. *Mechanical Systems and Signal Processing* 169:108620.

Please cite this article as: O.B. Ozdoganlar et al., Tchebychev-based modal-domain coupling (TMDC) for prediction of microtool-tip dynamics, CIRP Annals - Manufacturing Technology (2026), https://doi.org/10.1016/j.cirp.2026.04.054